

Electron transfer dissociation of multiply protonated and fixed charge disulfide linked polypeptides

Harsha P. Gunawardena^a, Lev Gorenstein^b, David E. Erickson^a,
Yu Xia^a, Scott A. McLuckey^{a,*}

^a Department of Chemistry, 560 Oval Drive, Purdue University, West Lafayette, IN 47907-2084, United States

^b Markey Center for Structural Biology, 915 West State Street, Purdue University, West Lafayette, IN 47907-2084, United States

Received 29 November 2006; received in revised form 24 January 2007; accepted 25 January 2007

Available online 3 February 2007

Abstract

Multiply protonated disulfide linked peptides and fixed charged analogs have been subjected to electron transfer ion/ion reactions to examine the role of excess protons in inducing cleavage of the disulfide bond in electron transfer dissociation. Systems in which all of the excess charge was due to fixed charge sites (i.e., quaternary ammonium groups) showed somewhat more disulfide bond cleavage than the fully protonated species. This observation argues against a major role for a mechanism that requires hydrogen transfer to the disulfide bond as a prerequisite for its cleavage. Interestingly, species with mixed cation sites (one or more excess protons and one or more fixed charge side chains) showed lower propensities for disulfide bond cleavage than either the corresponding fully protonated or fully derivatized species. This observation is not likely to be accounted for by direct electron transfer to a Coulomb stabilized disulfide bond because the identities of the charge bearing sites are not expected to play a significant role in the degree of stabilization. The results appear to be best rationalized on the basis of the ‘through bond electron transfer’ mechanism of Simons et al., in conjunction with rate limiting intramolecular electron transfer(s) between charge bearing sites. Intramolecular electron transfer between charge sites can play a role in mediating electron movement from the site of initial electron capture to the site from which an electron is transferred to the disulfide anti-bonding orbital.

© 2007 Elsevier B.V. All rights reserved.

Keywords: Electron transfer dissociation; Lysine fixed charge derivatives; Disulfide bonds; Ion/ion reactions

1. Introduction

Disulfide linkages in polypeptides are post-translational modifications that play a pivotal role in maintaining higher order structure and biological function. Characterization of primary amino acid sequence of disulfide linked peptides by mass spectrometry is typically performed by solution phase chemical reduction of the disulfide bond followed by alkylation of the thiol group [1]. The requirement for such sample manipulation prior to mass spectrometry has led to an interest in reducing disulfide linkages directly in the gas phase. It has been demonstrated that the disulfide linkage in polypeptides can be fragmented by several gas-phase methods. Collision-induced dissociation (CID) [2,6], electron capture dissociation (ECD)

[3], and UV photodissociation resulting in photochemical cleavage directly in the gas phase [4,5] or in MALDI matrices [6] as means of studying disulfide polypeptides and proteins have been reported. Fragmentation analogous to ECD has been demonstrated via gas-phase electron transfer reactions from singly charged anions to multiply protonated peptides. The dissociation resulting from electron transfer ion/ion reactions has been named electron transfer dissociation (ETD) [7,8]. Recently, preferential cleavage of the disulfide bond in several model peptides has also been investigated by electron transfer dissociation (ETD) [9]. ETD and ECD, therefore, may find use as means for cleaving disulfide bonds in gaseous polypeptides in the characterization of peptide and protein structures.

The mechanism for specific cleavage of disulfide bonds in peptides, proteins, and their analogs via ECD or ETD is an active area of research [10,11]. Several hypotheses have been put forth to explain the mechanism by which a disulfide bond is cleaved via ECD and the more recently developed ETD. An

* Corresponding author. Tel.: +1 765 494 5270; fax: +1 765 494 0239.
E-mail address: mcluckey@purdue.edu (S.A. McLuckey).

early proposal involved a so-called hot hydrogen model for electron capture dissociation [12]. The model essentially postulates the capture of an electron at a positive site, such as a protonated amine group, that releases a relatively energetic hydrogen atom that is eventually captured at a site of high hydrogen atom affinity, such as a disulfide bond (SS). Molecular dynamics calculations have since been used to conclude that the capture of “hot hydrogen atoms” is unlikely and that low energy hydrogen atoms are more likely to induce disulfide bond cleavage [13]. Alternatively, electron attachment to a charged site that is solvated by a nearby disulfide bond has also been proposed, whereby electron capture proceeds via hydrogen ion migration [8]. The mechanisms just mentioned involve a hydrogen species from a charged site that produces cleavages at a disulfide bond leading to $-S^{\bullet}$ and $-SH$ species. Calculations have also examined the possibility for dissociative electron attachment of disulfide bonds at low electron energies. The cross section for such a process in neutral molecules has been found to be extremely low due to a negative electron affinity associated with the disulfide linkage. Direct electron attachment at disulfide bonds in ions, however, has been shown to be plausible by virtue of the electrostatic contribution of nearby positive charge(s) in rendering exothermic the electron attachment to the disulfide bond [14,16]. This “coulomb assisted dissociation model” has also been applied to amide bond cleavage independently by Simons and co-workers [15] and by Syrstad and Tureček [16]. The Simons work has used Landau–Zener formalism [17,18] for electron transfer to estimate the likelihood for electron transfer both to backbone and disulfide bond sites [19,20]. In addition to direct electron capture/transfer, an alternative mechanism, referred to as “through bond electron transfer” has also been examined [21], whereby the electron is initially transferred to a Rydberg orbital of the cationic site from which it is transferred to an anti-bonding orbital of either the disulfide bond, leading to disulfide bond cleavage, or an amide unit on the backbone, leading to $N-C_{\alpha}$ bond cleavage.

ECD experiments described at a meeting involving fixed charge groups in non-disulfide linked peptides have shown backbone cleavage, thereby suggesting that hydrogen atoms may not be essential to the formation of c and z-type ions [22]. Also, disulfide linked peptides carrying excess alkali cations instead of protons have shown disulfide bond cleavage upon electron capture. In this study, attention has been focused on the ETD of several model disulfide linked polypeptide ions in which the partitioning of the ion/ion reaction products between the various possible channels is carefully monitored. Of particular interest is the comparison of ETD behavior for ions in which the net charge is accounted for by either excess protons or by fixed charge sites (i.e., quaternary ammonium cations). The latter ions are expected to be much less likely, upon transfer of an electron, to provide a hydrogen atom to induce cleavage of a disulfide bond than the multiply protonated analogs. Calculations have also been performed to determine if the electron affinity of the disulfide bond associated with a model system examined here is sufficiently large to render exothermic electron transfer to the disulfide linkage.

2. Experimental

2.1. Materials

Azobenzene was purchased from Sigma–Aldrich (St. Louis, MO). Somatostatin was purchased from AnaSpec (San Jose, CA). TPCK-treated trypsin was purchased from Worthington Biochemical Cooperation (Lakewood, NJ).

2.2. Tryptic digestion

Somatostatin (0.5 mg) was dissolved to a volume of 0.5 ml of aqueous 20 mM ammonium bicarbonate. TPCK-treated trypsin (2 μ l of a 1 mg/ml aqueous solution) was added to the peptide solution to effect digestion, for variable time periods ranging from 5 min to 2 h at 37 °C to obtain either partial or complete digestion. After digestion, the samples were fractionated by reversed-phase HPLC, as described further below.

2.3. Peptide fixed charge derivatization

Fixed charge derivatization [23,24] was carried out using the *N*-hydroxysuccinimide ester of 4-trimethylammonium butyrate (NHS-TMAB) reagent, a gift from Prof. Fred Regnier. The NHS-TMAB reagent was prepared to a concentration of 1 mg/ml in a sodium borate solution buffered at pH \sim 9. The NHS-TMAB reagent solution (500 μ l) was added to the dried digested somatostatin peptides. The reaction was allowed to proceed for 2 h at room temperature. The acylation reaction was quenched by adding 1–2 drops of acetic acid and the reaction mixture was purified using a reversed-phase HPLC.

2.4. Methyl esterification

A solution of 2N HCL in methanol was prepared at room temperature by the drop-wise addition of 400 μ l acetyl chloride to 2.5 ml of anhydrous methanol with stirring in an ice bath. After 5 min, 100 μ l of this reagent was added to the dried peptide. The reaction was allowed to proceed for 2 h at room temperature and then the sample was dried in vacuum.

2.5. Liquid chromatographic separation

All liquid chromatographic (LC) experiments were carried out on an Agilent HPLC (model 1100, Santa Clara, CA), using a Poros (Applied Biosystems, Foster City, CA) R1/10 100 mm \times 2.1 mm i.d. column operated at 1 ml/min. A linear 20-min gradient from 0 to 100% B was used, where buffer A was 0.1% aqueous TFA and buffer B was 60% acetonitrile/40% H₂O containing 0.09% aqueous TFA. The fractions were dried in vacuum.

The two tryptic peptide sequences and their derivatives are listed as peptides I–X in Table 1. Peptides II–V are modified forms of peptide I and peptides VII–X are modified forms of peptide VI. For all peptides, the A-chain refers to the chain with alanine as the N-terminus whereas the B-chain refers to the chain with threonine as the N-terminus.

2.6. Mass spectrometry

Experiments were performed using a commercial quadrupole/time-of-flight tandem mass flight spectrometer (QSTAR XL, Applied Biosystems/MDS SCIEX, Concord, Ont., Canada), modified to allow for ion/ion reactions studies [25]. A home-built pulsed dual source [26] was coupled directly to the nanospray interface of the QSTAR instrument, comprising a nanospray emitter for the formation of positive peptide ions ($[M + nH]^{n+}$) and an atmospheric pressure chemical ionization (APCI) needle for the formation of radical anions from the electron transfer reagents. Electron transfer ion/ion reactions were implemented in the Q2 linear ion trap (LIT) via superposing auxiliary radio frequency (rf) signals (120 kHz, 150 V) on the end lenses of the Q2 LIT to enable mutual storage of oppositely charged ions. The pressure in Q2 was approximately 5 mTorr with nitrogen as a bath gas. The experimental procedure for the electron transfer ion/ion reactions used here has been reported in detail elsewhere [25]. In brief, a typical scan function consisted of steps as follows: (1) anion injection into Q2 LIT with Q1 quadrupole in mass-resolving mode to isolate the reagent ions of interest (200 ms); (2) positive ion injection into Q2 LIT with Q1 quadrupole in mass-resolving mode to isolate analyte ions of interest (50 ms); (3) mutual cation/anion storage in Q2 LIT (50 ms); (4) mass analysis by a reflectron time-of-flight (TOF) (50 ms). The TOF analyzer typically provided a mass resolution of 6000–8000 and mass accuracy of ~ 50 ppm (external calibration). The mass spectra shown here are the averages of 50–100 individual scans.

2.7. Calculations

High level density functional theory (DFT) and *ab initio* computations were carried out to obtain the structures and energies of ions and neutral species relevant to this study using Gaussian 03 [27]. Geometry optimizations, including vibrational analysis, were performed at B3LYP/6-31+G(d)

level. All stationary points were found to be true minima by carrying out vibrational frequency analysis using the same basis set [28,29]. To determine the energies of the various species, single-point energy calculations were performed using B3LYP/aug-cc-PVTZ. Molecular mechanics calculations were performed using the MacroModels AMBER* force field [30]. The peptide X (see Table 1) modified at both N termini and the lysine residues was used in all computations. Adequate conformational sampling was achieved by a combination of multiple simulated annealing and constant temperature molecular dynamics (MD), similar to the approach described earlier [31]. The *in vacuo* ($\epsilon = 1$) simulated annealing procedure was carried out where the initial structure was subjected to a molecular dynamic run from 800 to 1 K for 25 ps with 1 fs time step followed by energy minimization with truncated newton conjugated gradient (TNCG) numerical method to the gradient of ≤ 0.05 kJ/mol Å. The resulting structure was stored and used as a starting point for the next annealing cycle. Simulated annealing cycles were repeated to produce 200 structures of which the 10 lowest energy structures were selected. Selected structures were subjected to a short 25 ps MD equilibration, followed by a 1 ns production MD run. Both equilibration and production MD were performed at a constant bath temperature of 300 K with a 1 fs time step and 25 ps sampling interval. The distance from each of the four fixed charge groups to the center of the peptide SS bond was monitored during the simulation.

3. Results and discussions

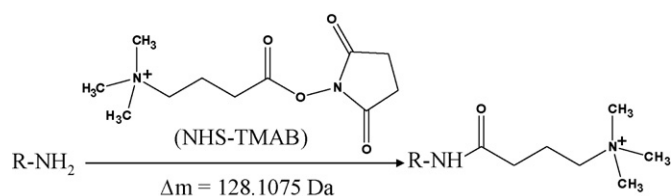
Complete digestion of somatostatin with TPCK-treated trypsin yields peptide I as one of its fragments. The primary amine groups associated with the N-termini of the two peptide chains linked via a disulfide bond as well as the amine group of the lysine residue can be converted to fixed positive charge sites of the form indicated in Scheme 1.

The species formed from conversion of one of the primary amine groups to a fixed charged site is referred to as peptide

Table 1
Peptide sequences

Peptide label	Peptide sequence	Peptide label	Peptide sequence
Peptide I	AGCK TFTSC	Peptide VI	AGCKNFWK TFTSC
Peptide II* (with one TMAB)	AGCK TFTSC	Peptide VII* (with one TMAB)	AGCKNFWK TFTSC
Peptide III* (with two TMAB)	AGCK TFTSC	Peptide VIII* (with two TMAB)	AGCKNFWK TFTSC
Peptide IV	(q)AGCK(q) (q)TFTSC	Peptide IX* (with three TMAB)	AGCKNFWK TFTSC
Peptide V	(q)AGCK(q)-OMe (q)TFTSC-OMe	Peptide X	(q)AGCK(q)NFWK(q) (q)TFTSC

TMAB modification is denoted as (q). Asterisk (*) represents that the peptides have a mixture of structures with combinations of TMAB on N-termini or lysine side chains.



Scheme 1. Reaction scheme of charge derivatization on a primary amine group of a peptide using reagent *N*-hydroxysuccinimide ester of 4-trimethylammonium butyrate (NHS-TMAB).

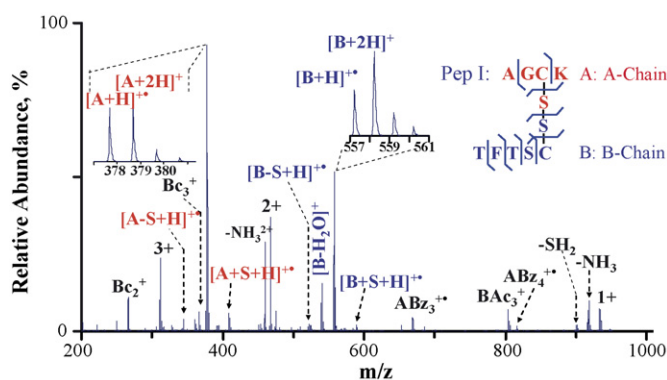


Fig. 1. Spectrum derived from the ion/ion reaction involving azobenzene radical anions and the $[M+3H]^{3+}$ ion of peptide I, denoted as 3+ in the figure.

II, which is expected to be a mixture of peptides with the fixed charge site present at any of the three possible locations. Peptide III is the species formed from derivatization of two of the three primary amine groups and is also expected to be comprised of a mixture of isomeric ions. Conversion of all of the primary amine groups to fixed charge sites is referred to herein as peptide IV. Methyl esterification of the C-termini of peptide IV yields peptide V. Figs. 1–3 compare the results obtained for the reaction of the 3+ ions of peptides I, IV, and V with the radical anion of azobenzene. The charge of the peptide I ions results from three excess protons whereas those of the peptides IV and V ions result from the presence of three quaternary ammonium fixed charge sites.

As in the previous ETD study of disulfide linked peptides, we use the notation ABm_n for backbone cleavages to specify

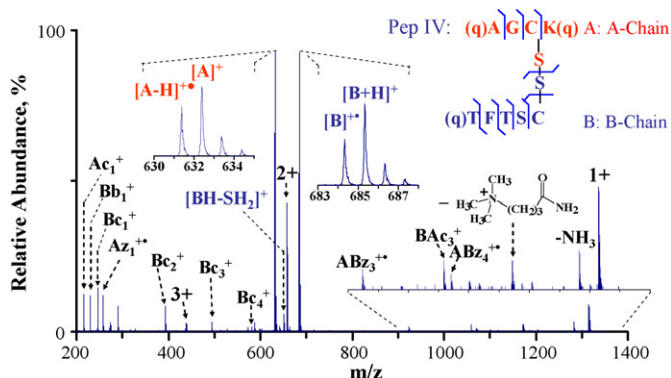


Fig. 2. Post-ion/ion reaction product ion spectrum derived from triply charged peptide IV with the azobenzene radical anion.

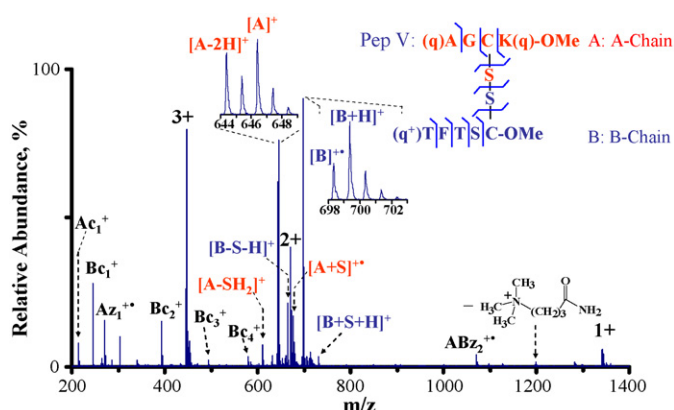
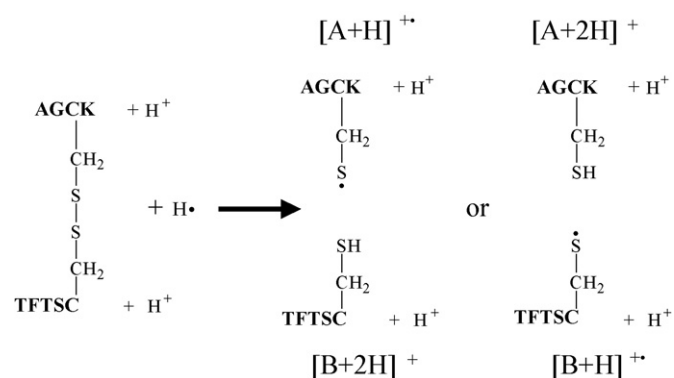


Fig. 3. Post-ion/ion reaction product ion spectrum derived from triply charged peptide V with the azobenzene radical anion.

that a product ion contains the full A-chain linked to the B-chain, which is cleaved so as to produce the m_n sequence ion. Alternately, BAm_n would indicate the full B-chain linked to the A-chain, which is cleaved so as to produce the m_n sequence ion. The sequence ions that are complementary to either ABm_n or BAm_n species do not contain the disulfide linkage and are therefore indicated by Ap_n or Bp_n , where p_n is the complement to the m_n fragment. In Fig. 1, evidence for the cleavage of a number of N–C $_{\alpha}$ bonds of peptide I is apparent and these are summarized in the figure insert. By far the major dissociation products, however, reflect cleavages along the disulfide linkage. As has been noted previously with ECD and ETD, cleavage of the disulfide linkage takes place primarily between the sulfur atoms. For triply protonated peptide I, the transfer of an electron initially produces a doubly charged ion that fragments into complementary singly charged ions (no doubly charged fragment ions that arise from disulfide cleavage are apparent in Fig. 1). If there is no H $^{\bullet}$ loss, cleavage of the S–S bond leads to the major complementary ions summarized in Scheme 2. (Note that plausible structures can also be drawn that do not require the formation of a hydrogen atom as part of the overall process. Also, the location of the radical site might also differ from those indicated in the scheme.) Fig. 1 shows evidence for both sets of complementary ion pairs indicated in the scheme, as has been noted in previous ECD and ETD studies. If it is assumed that two charges



Scheme 2. Complementary ion pairs formed from SS bond cleavage following electron transfer to the $[M+3H]^{3+}$ ion of peptide I.

are initially present on the A-chain in the $[M+3H]^{3+}$ ion, the formation of the $[A+2H]^+/[B+H]^{\bullet+}$ complementary pair does not require a hydrogen atom transfer between chains whereas the $[A+H]^{\bullet+}/[B+2H]^+$ pair requires the transfer of a hydrogen atom from the A-chain to the B-chain.

Fig. 2 shows the post-ion/ion reaction product ion spectrum of triply charged peptide IV following reaction with the azobenzene radical anion. Peptide IV was formed by conversion of the lysine residue and the two N-termini of peptide I to fixed charge sites. In this case, there are no nominally “excess” protons from which to form hydrogen radicals.

If the presence of a hydrogen radical is a prerequisite for SS bond cleavage in ETD, peptide IV might be expected to show a reduced tendency for such cleavage. However, it is clear from the spectrum that both N–C $_{\alpha}$ backbone bond and disulfide bond cleavages occur with this peptide ion, with SS bond cleavage being dominant. There is also evidence for a relatively minor cleavage of the doubly charged ion formed by electron transfer to yield a cation derived from the fixed charged side-chain, $H_2NCO(CH_2)_3N^+(CH_3)_3$, and its complementary ion. As with peptide I, two complementary ion pairs are observed with disulfide bond cleavage in peptide IV. Nominal structures associated with these complementary ion pairs are shown in Scheme 3 but these are not intended to preclude other variations. For example, in the $[A]^+$ ion, while a formal negative charge is shown on the sulfur atom in Scheme 3, it is also possible to indicate a thiol group and a deprotonated carboxyl terminus. All disulfide bond cleavage products were observed to be singly charged with the two complementary ion pairs indicated in Scheme 3, i.e., $[A-H]^{\bullet+}/[B+H]^+$ and $[A]^+/[B]^{\bullet+}$. The former complementary pair arises from the transfer of a hydrogen atom from the A-chain to the B-chain whereas the latter pair does not require hydrogen transfer.

While the results for peptide IV suggest that excess protons are not necessary for disulfide bond cleavage via ETD, the formation of a salt-bridge structure that could free the carboxylate proton is not precluded. Therefore, data were collected for peptide V, which is identical to peptide IV except that the two C-termini were methyl esterified. This modification precludes salt-bridge formation involving the C-termini. The results for the ETD experiment for the triply charged ion of peptide V

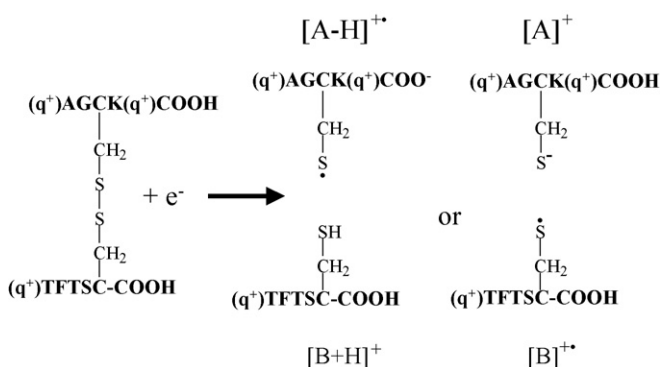
are shown in Fig. 3. As with the triply charged ions of peptides I and IV, ETD to give both backbone and disulfide bond cleavage is observed. Once again, disulfide bond cleavage dominates. Few differences are noted between the ETD behaviors of peptides IV and V, indicating that methyl esterification has little effect on disulfide bond cleavage. Perhaps the major phenomenon that appears to be unique to peptide V is the formation of a product consistent with $[A-2H]^+$, although a significant contribution of the complementary ion for this species (i.e., a $[B+2H]^{\bullet+}$ species) does not appear to be present with the ^{13}C $[B+H]^+$ ion. The origin of this ion was not investigated further. The $[A-H]^{\bullet+}/[B+H]^+$ and $[A]^+/[B]^{\bullet+}$ complementary pairs are both clearly apparent. The relative contribution of the $[A-H]^{\bullet+}/[B+H]^+$ pair, which involves a hydrogen transfer from the A to the B-chain, does not appear to be significantly lower for the peptide V ion than was noted for the peptide IV ion. This leaves open the question of the origin of the transferred hydrogen. An amide hydrogen is a possibility. The acidity of the amide group can be increased by interaction of the fixed charge side-chain with the carbonyl oxygen. In any case, it is clear that excess protons are not necessary for ETD, and more specifically, SS bond cleavage of disulfide linked peptides.

ETD data were also collected for the triply charged partially derivatized peptides II and III. These peptides are comprised of one (peptide II) or two (peptide III) fixed charged sites. Each population is expected to be a mixture of isomers with all of the possible combinations of fixed charge site locations. In both cases, evidence for disulfide bond cleavage as well as N–C $_{\alpha}$ backbone cleavages was noted. However, the relative contributions of disulfide bond cleavage were lower for these mixed charge bearing site peptides than for either peptide I (all excess protons) or peptides IV and V (all fixed charge sites), as discussed further below.

It is of interest to examine the partitioning of the ion/ion reaction products between the various major reaction pathways. For all ion/ion reactions involving peptide cations, proton transfer can compete with electron transfer. Proton transfer from the $[M+3H]^{3+}$ peptide I ion yields the $[M+2H]^{2+}$ ion. No fragmentation due to ion/ion proton transfer is observed. Electron transfer that does not result in fragmentation leads, in the case of the $[M+3H]^{3+}$ ion of peptide I, to the $[M+3H]^{\bullet 2+}$ species, which can be distinguished from the proton transfer product due to the 1 Da mass difference. Electron transfer can lead to dissociation, which, in the case of peptide I, gives rise to peptide backbone bond cleavage, disulfide bond cleavage, and side-chain cleavage products. (Note that electron transfer followed by loss of H^{\bullet} cannot be distinguished from proton transfer.) The partitioning between proton transfer (%PT), electron transfer without dissociation (%ET, no D), and electron transfer dissociation (%ETD) is given by relationships (1)–(3):

$$\%PT = \frac{\sum PT}{\sum PT + (ET, \text{no D}) + ETD} \times 100 \quad (1)$$

$$\%ET, \text{no D} = \frac{\sum ET, \text{no D}}{\sum PT + (ET, \text{no D}) + ETD} \times 100 \quad (2)$$



Scheme 3. Complementary ion pairs formed from SS bond cleavage following electron transfer to the triply charged ion of peptide IV.

Table 2

Ion/ion reaction product partitioning for various peptide cations in reaction with the azobenzene radical anion

Peptide	%ETD	%ET, no D	%PT	%SS/ETD
3+ peptide ions react with azobenzene anions				
Peptide I	83 ± 0.8	2 ± 0.7	15 ± 0.6	71 ± 2
Peptide II	82 ± 6	0.2 ± 0.1	18 ± 6	68 ± 4
Peptide III	52 ± 11	9 ± 3	39 ± 7	36 ± 4
Peptide IV	68 ± 12	0.6 ± 0.2	31 ± 12	80 ± 2
Peptide V	74 ± 1	1 ± 0.7	25 ± 9	73 ± 2

$$\%ETD = \frac{\sum ETD}{\sum PT + (\sum ET, \text{no D}) + ETD} \times 100 \quad (3)$$

where $\sum ETD$ products includes all products from backbone cleavage, side chain cleavage, and disulfide bond cleavage, $\sum PT$ is the sum of the proton transfer products, and $\sum ET, \text{no D}$ is the sum of the electron transfer products that do not undergo subsequent fragmentation. Note that these relationships do not include the residual reactant ion population, as these ions are not relevant to the determination of the partitioning of ion/ion reaction products. In the case of disulfide linked peptides, it is also of interest to determine the disulfide bond cleavage as a percentage of the total extent of ETD, as represented by relation (4).

$$\frac{\%SS}{ETD} = \frac{\sum SS \text{ products}}{\sum ETD} \times 100 \quad (4)$$

The partitioning of ion/ion reaction products for the ions formed from peptides I–V is summarized in Table 2. In the cases of peptides I, II, IV, and V, very little electron transfer without dissociation (0–3%) was apparent in the isotope distributions of the doubly charged intact ion/ion reaction products. Peptide III showed a somewhat greater degree of electron transfer without dissociation (9%). Peptide I gave the lowest relative contribution of proton transfer (15%), while higher contributions were noted for all other fixed charge derivatives. Peptide III showed the greatest degree of proton transfer with a %PT of 39%. Consequently, while there was little variation in %ETD for four of the five peptide ions, peptide III ions showed a lower %ETD value (viz., 52% versus 74–82% for the other peptide ions). Perhaps the most striking behavior is apparent in the fraction of ETD products represented by disulfide bond cleavage, as reflected in the %SS/ETD values. There is a greater %SS/ETD for peptide IV than for peptide I, which is accounted for by a decrease in the relative contribution of backbone bond cleavages. The relative decrease in backbone cleavages is actually masked to some degree in the %SS/ETD values by the appearance of products due to loss of the fixed charge side chain, which is observed in peptides IV and V, and contributes to the denominator in the calculation of %SS/ETD. (These channels, however, make only minor contributions.) However, the most noteworthy observation in the comparison of the various %SS/ETD values is the lower tendency for disulfide bond cleavage in the mixed charge site ions. In particular, peptide III, with two fixed charge sites and one excess proton, shows a %SS/ETD value of only

Table 3

Ion/ion reaction product partitioning for various peptide cations in reaction with the azobenzene radical anion

Peptide	%ETD	%ET, no D	%PT	%SS/ETD
4+ peptide ions react with azobenzene anions				
Peptide VI	87 ± 4	3 ± 1	10 ± 3	32 ± 3
Peptide VII	73 ± 1	9 ± 0.2	18 ± 0.8	40 ± 1
Peptide VIII	68 ± 8	8 ± 2	24 ± 6	23 ± 3
Peptide IX	50 ± 4	14 ± 4	36 ± 1	6 ± 0.5
Peptide X	63 ± 0.6	10 ± 0.7	27 ± 1	64 ± 0.8

36%, whereas the values for the other peptides were 68% or greater.

The partitioning between proton transfer, electron transfer without dissociation, ETD of backbone bonds, and ETD of disulfide bonds may depend upon a number of variables, which include characteristics of both the anionic reagent and the polypeptide ion. For example, in the case of the anion, the Franck–Condon factors associated with the transition from anion to neutral and the electron affinity of the neutral play important roles in determining the outcome of the competition between proton transfer and electron transfer [32]. For this work, we emphasized use of the azobenzene radical anion, a species that we have found to maximize electron transfer relative to proton transfer. The characteristics of the cation that affect the partitioning among the various channels in an ion/ion reaction are less well characterized. However, the degree of electrostatic repulsion in the cation is apparently particularly important in determining the relative contributions of ET, no D versus ETD and, perhaps, proton transfer versus electron transfer [33]. Other possible variables may be the identities of the charge bearing sites, the degree of intramolecular hydrogen bonding, etc. It is beyond the scope of this work to explore all of these variables. However, it is clear that there is significant variation in the ion/ion product ion partitioning in the comparison of peptides I–V, particularly for peptide III. We have therefore examined a related disulfide linked polypeptide and its variants (i.e., peptides VI–X) to compare the partitioning of ion/ion products with peptides I–V.

Fig. 4 compares the post-ion/ion reaction data for quadruply protonated peptide VI, the 4+ mixed cation peptide IX (three fixed charge sites and one excess proton), and the 4+ ion of the fixed charged derivative peptide X (four fixed charge sites). The ion/ion reaction product partitioning among the various categories defined in relations (1)–(4) for these ions, along with those obtained for the 4+ ions of peptides VII and VIII, is given in Table 3. In all cases, disulfide bond cleavage was noted in which the A-chain ions carried two charges and the B-chain products were always singly charged. Overall, the 4+ ions of peptides VI–X yielded %PT and %ET, no D values comparable to the analogous triply charged peptides I–V. The %SS/ETD values, on the other hand, were consistently lower. This may simply be due to the fact that there are more possible N–C α bond cleavages to compete with disulfide bond cleavage in peptides VI–X than in peptides I–V. However, similar trends within each peptide group (i.e., trends within the peptides I–V and peptides VI–X data sets) were noted. In particular, it is noteworthy that

the 6% value of %SS/ETD for peptide IX (three fixed charges and one excess proton) is significantly lower than for any of the other peptides in the group. This is consistent with the low relative %SS/ETD observed for peptide III (one excess proton with the remainder of the charge due to fixed charges). Also, for each peptide group, the species that shows the greatest degree of disulfide bond cleavage upon ETD is the species in which all of the charge can be ascribed to the fixed charge modification (i.e., peptides VI, V, and X).

It is of interest to consider the implications of the results described above on mechanistic aspects of the ETD of disulfide linked polypeptide cations. If the formation of a hydrogen atom from a protonated amine site is essential for the major mechanism for disulfide bond cleavage, a noticeable difference in behavior might be expected in the comparisons of peptides I, IV, and V and peptides VI and X. In particular, a decrease in disulfide linkage cleavage might be expected as the identities of the charge bearing sites change from protonated amine groups to quaternary ammonium groups. The fact that no such decrease was observed, and the fact that the %SS/ETD values actually increase in the fixed charge peptides, calls into question the need for hydrogen atom interaction with the disulfide linkage as a rate-determining process. However, the fixed charge peptide experiment does not necessarily preclude the possibility

that hydrogen atoms are involved in the process. The fact that hydrogen transfer from one chain to the other is observed for some of the disulfide bond cleavages, even for the fixed charge peptides, indicates a degree of hydrogen atom mobility in the ions prior to separation of the chains. It is not clear, however, if hydrogen transfer occurs prior to or after cleavage of the disulfide bond. On the other hand, disulfide linkage cleavage that does not lead to hydrogen atom transfer between the side-chains is a major process, even for the multiply protonated forms of the peptides. Hence, it is apparent that the presence of an “excess proton”, resulting from protonation of basic side chains or the N-termini, is neither a prerequisite for disulfide bond cleavage nor does it appear to make a major difference either way for the systems studied here. The trend toward greater %SS/ETD values in fixed charge species relative to multiply protonated species, however, may imply that in the case of backbone cleavages, the presence of excess protons does make a significant difference.

While dissociation studies of this type can provide only indirect mechanistic evidence, the data reported here appear to be consistent with proposals made by Simons et al. regarding disulfide linkage cleavage in ETD. These proposals include either direct electron capture into an anti-bonding orbital of the SS bond, which is made energetically favorable by the Coulomb stabilization afforded by the surrounding positive charge, or initial capture into a Rydberg state of the charge site with subsequent transfer into the anti-bonding orbital of the disulfide bond. (Note that recent evidence for extensive radical migration in ECD [34–36], which presumably takes place over much longer time-frames than intramolecular electron transfer, suggests that the lifetime of the species initially formed upon ion/ion electron transfer is sufficiently long-lived to allow for intramolecular electron transfer.) Proton transfer to the anionic SS site could lead to disulfide bond cleavage or direct cleavage of the anionic SS bond with or without subsequent proton transfer are also possibilities. The fact that the tendency for SS bond cleavage is not significantly perturbed by converting the peptide to fixed charge species would appear to indicate either that proton transfer is equally facile from sites on the polypeptide other than protonated side chains or the N-termini or that proton transfer to the disulfide bond is not a prerequisite for cleavage.

The behaviors of the mixed charge site species, particularly peptides III and IX, are intriguing because they indicate that there is not a simple trend for any of the parameters given by relations (1)–(4) based on the number of excess protons. The cases in which only one excess proton is present, for example, give rise to the lowest contributions from SS bond cleavage to the total ETD. Within the context of the mechanisms proposed to date for disulfide bond cleavage from ECD and ETD (viz., hydrogen transfer from a neutralized protonated site, direct electron capture by the disulfide bond, and electron transfer to an anti-bonding orbital of the SS bond from a Rydberg state of a neutralized charge site), the scenario that best accounts for the observed behavior involves intra-ion electron transfer. As discussed above, it seems unlikely that a mechanism that requires hydrogen transfer to the disulfide bond to induce dis-

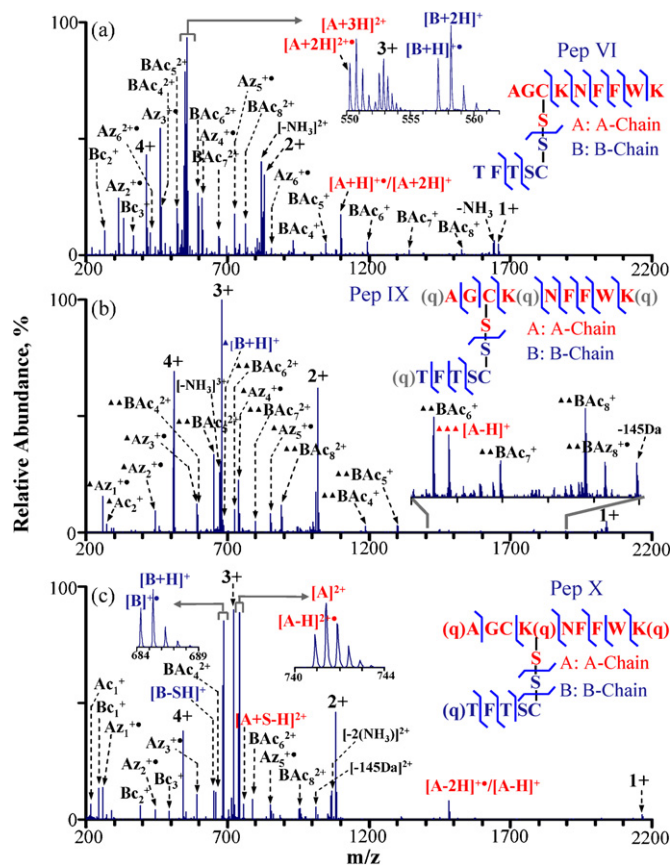


Fig. 4. Post-ion/ion reaction product ion spectra derived from (a) quadruply protonated peptide VI, (b) quadruply charged peptide IX (three fixed charge sites and one excess proton), and (c) quadruply charged peptide X (four fixed charge sites) with the azobenzene radical anion. In (b) the number of the filled triangles represents the number of TMAB groups on the product ions.

sociation can readily account for all of the observed behavior. It also seems unlikely that significant variations in %SS/ETD should be expected within the peptide I–V and peptide VI–X groupings if direct electron capture at the disulfide linkage is the major mechanism because the overall Coulomb fields are expected to be similar. Certainly, there is no reason to expect that the peptide ions with mixed charge site identities should result in a lower propensity for direct electron capture at the disulfide linkage. However, a mechanism that involves initial electron transfer to one charge site with subsequent electron transfer(s) to eventually populate the anti-bonding orbital of the disulfide bond might account for the lower %SS/ETD values associated with the peptide ions with mixed charge site identities. According to the “through bond electron transfer model” of Simons et al., the distance from the site of electron capture to the disulfide bond is a key factor in determining the probability of electron transfer. (Note that a “through space electron transfer” process would also be consistent with these data.) It is important to recognize, therefore, that the initial site of electron capture (either of a free electron or an electron from negative reagent ion) may not be the site with the most favorable probability for electron transfer to the disulfide bond. If intra-molecular electron transfer between charge bearing sites is slow, as might be the case for dissimilar charge bearing sites (e.g., a quaternary ammonium cation versus a protonated amine), disulfide bond cleavage may not be observed if the site of initial transfer/capture is remote from the disulfide bond. Hence, we speculate that the lower relative %SS/ETD values for the peptides with mixed cation sites might arise from the fact that initial electron transfer to the cation may not populate the charge bearing sites with highest probability for electron transfer to the disulfide bond. Furthermore, the subsequent electron transfer from the initial capture site to the site that transfers an electron to the disulfide bond is a rate determining step and that there are lower rates of electron transfer between dissimilar charge bearing sites than for the similar ones. Such a scenario could account for a lower fraction of electron capture events giving rise to disulfide bond cleavage.

Both the direct electron capture/transfer and through bond electron transfer mechanisms described above require that electron binding at the disulfide linkage be energetically favorable. For neutral disulfide bonds, electron binding is energetically unfavorable by roughly 1 eV [37]. To determine if electron binding to the disulfide bond in the peptides studied here is likely to be favorable, we estimated the electron binding energy of the disulfide linkage of peptide X via relation (5) [14]:

$$-EA_{SS-ion} \text{ (eV)} = -EA_{SS-neutral} \text{ (eV)} - 14.4 \text{ (eV)} \sum_j R_j^{-1} \quad (5)$$

where $-EA_{SS-ion}$ (eV) is the binding energy (or the negative of the electron affinity) of the electron at the SS bond in the ion, $-EA_{SS-neutral}$ (eV) is the negative of the electron affinity of the SS bond in the absence of a positively charged environment, and the last term accounts for the sum of the pair-wise stabilizing electrostatic interactions between the j th positive site of distance R_j from the midpoint of the SS bond. The latter term of relation

(5) represents the Coulomb stabilization of an electron located at the disulfide bond. Molecular dynamics calculations were used to estimate the R_j values for peptide X. Similar Coulomb stabilization energies of approximately -3.3 eV were found for the lowest energy structures obtained in the MD simulations, which translates to an EA_{SS-ion} of 2.3 eV for the 4+ ion of peptide X. After neutralization of the closest fixed charge site, the EA_{SS-ion} remains positive at 1.3 eV. The former value is relevant for direct electron transfer to the disulfide bond whereas the latter value is relevant for the “through bond electron transfer” mechanism. The EA of the Rydberg nitrogen orbital of a quaternary ammonium group was calculated to be approximately 2.7 eV while Coulomb stabilization by the presence of nearby charges in the +4 peptide V ion increases the EA values of all of the charge sites to 4–5 eV. The EA values of the species used to form anions in this work are well below 2.7 eV (e.g., azobenzene EA = 0.5 eV [38]) which makes possible both the direct electron transfer to the SS bond of 4+ peptide V and transfer to the Rydberg orbital with subsequent transfer to the SS bond. The use of a reagent anion with an EA value greater than 2.7 eV might be an interesting experiment because it might allow for the distinction between the two potential processes. However, high electron affinity species tend to undergo proton transfer. Hence, this competing ion/ion reaction channel represents a significant challenge to such an experiment.

4. Conclusions

Electron transfer ion/ion reactions between protonated disulfide linked peptides and their fixed charge analogs have been studied. Ion/ion product ion partitioning between proton transfer, electron transfer without dissociation, ETD, and the fraction of ETD arising from disulfide bond cleavage was recorded. The relative contribution to the total ETD noted for these peptides is reported as %SS/ETD. This measure is defined as the total product ion intensity resulting in the dissociation of the SS bond normalized to the total ETD product ion abundance. For the systems studied, the %SS/ETD values found for the fully protonated versions of the peptides were slightly smaller than those where all charges were due to fixed charge derivatives (i.e., no nominally excess protons present). This observation suggests that mechanisms that require hydrogen transfer to the disulfide linkage as a prerequisite for cleavage are not likely to be the dominant processes for these ions. This observation may also have implications for the relative propensity for backbone cleavages, as the %SS/ETD value reflects the competition between disulfide bond cleavage and backbone cleavage. Interestingly, peptides with mixed charge site identities (i.e., those with one or more fixed charge sites as well as one or more excess protons) show lower %SS/ETD values than either the fully protonated or fully derivatized versions of the same peptide ion. Of the mechanisms currently put forth for disulfide bond cleavage in polypeptide cations via ETD, a process that involves the ‘through bond electron transfer’ mechanism appears to be best able to accommodate the observations made in this work. The systems studied here may highlight the importance of intra-molecular electron transfer between charge bearing sites. The site of initial

electron capture may not be the site most readily capable of transferring an electron to the disulfide anti-bonding orbital. Hence, the propensity for electron transfer between charge bearing sites may play a role in the competition between disulfide bond cleavage and backbone cleavage. Future studies will employ mixed cation site systems in which the locations of each charge site type are defined.

Acknowledgment

This work was supported by the Office of Basic Energy Sciences, Division of Chemical Sciences under Award No. DE-FG02-00ER15105.

References

- [1] J.J. Gorman, T.P. Wallis, J.J. Pitt, *Mass Spectrom. Rev.* 21 (2002) 183.
- [2] J.A. Loo, C.G. Edmonds, H.R. Udseth, R.D. Smith, *Anal. Chem.* 62 (1994) 693.
- [3] R.A. Zubarev, D.M. Horn, E.K. Fridricksson, N.L. Kelleher, M.A. Lewis, B.A. Carpenter, F.W. McLafferty, *Anal. Chem.* 72 (2000) 563.
- [4] Y.M.E. Fung, F. Kjeldsen, O.A. Silvira, T.W.D. Chan, R.A. Zubarev, *Angew. Chem. Int. Ed.* 44 (2005) 6399.
- [5] C.W. Bookwalter, D.L. Zoller, P.L. Ross, M.V. Johnston, *J. Am. Soc. Mass Spectrom.* 6 (1995) 872.
- [6] Y. Fukuyama, S. Iwamoto, K. Tanaka, *J. Mass Spectrom.* 41 (2006) 191.
- [7] J.E.P. Syka, J.J. Coon, M.J. Schroeder, J. Shabanowitz, D.F. Hunt, *Proc. Natl. Acad. Sci. U.S.A.* 101 (2004) 9528.
- [8] J.J. Coon, J.E.P. Syka, J. Shabanowitz, D.F. Hunt, *Int. J. Mass Spectrom.* 236 (2004) 33.
- [9] P.A. Chrisman, S.J. Pitteri, J.M. Hogan, S.A. McLuckey, *J. Am. Soc. Mass Spectrom.* 16 (2005) 1020.
- [10] E. Uggerud, *Int. J. Mass Spectrom.* 234 (2004) 45.
- [11] F. Tureček, M. Polášek, A.J. Frank, M. Sadílek, *J. Am. Chem. Soc.* 122 (2000) 2361.
- [12] R.A. Zubarev, N.L. Kelleher, F.W. McLafferty, *J. Am. Chem. Soc.* 120 (1998) 3265.
- [13] V. Bakken, T. Helgaker, E. Uggerud, *Eur. J. Mass Spectrom.* 10 (2004) 625.
- [14] A. Sawicka, P. Skurski, R.R. Hudgins, J. Simons, *J. Phys. Chem. B* 107 (2003) 13505.
- [15] I. Anusiewicz, J. Berdys-Kochanska, J. Simons, *J. Phys. Chem. A* 109 (2005) 5801.
- [16] E.A. Syrtstad, F. Tureček, *J. Am. Soc. Mass Spectrom.* 16 (2004) 208.
- [17] L.D. Landau, *Phys. Z (USSR)* 2 (1932) 46.
- [18] C. Zener, *Proc. Royal Soc. (London) A* 136 (1932) 696.
- [19] M. Sobczyk, J. Simons, *J. Phys. Chem. B* 110 (2006) 7519.
- [20] I. Anusiewicz, J. Berdys-Kochanska, J. Simons, *J. Phys. Chem. A* 110 (2006) 1261.
- [21] M. Sobczyk, J. Simons, *Int. J. Mass Spectrom.* 253 (2006) 274.
- [22] R.R. Hudgins, K. Håkansson, J.R. Quinn, C.L. Hendrickson, A.J. Marshall, *Proceedings of the 50th Annual Conference on Mass Spectrometry and Allied Topics*, Orlando, FL, 2002.
- [23] R.M. Johnson, S.A. Martin, K. Biemann, *Int. J. Mass Spectrom. Ion Processes* 86 (1998) 137.
- [24] H. Mirzaei, F.E. Regnier, *Anal. Chem.* 78 (2006) 4175.
- [25] Y. Xia, P.A. Chrisman, D.E. Erickson, J. Liu, X. Liang, F.A. Londry, M.J. Yang, S.A. McLuckey, *Anal. Chem.* 78 (2006) 4146.
- [26] X. Liang, Y. Xia, S.A. McLuckey, *Anal. Chem.* 78 (2006) 3208.
- [27] J.A. Pople, et al., *Gaussian, Inc.*, Pittsburgh, PA, 2003.
- [28] L.A. Curtiss, K. Raghavachari, G.W. Trucks, J.A. Pople, *J. Chem. Phys.* 94 (1991) 7221.
- [29] J.B. Foresman, E. Frisch, *Exploring Chemistry with Electronic Structure Methods*, 2nd ed., Gaussian, Pittsburgh, 1996.
- [30] *MacroModel*, Version 9.0, Schrödinger, LLC, New York, NY 2005.
- [31] M.C. Polfer, K.F. Haselman, P.R.R. Landrige-Smith, P.E. Barran, *Mol. Phys.* 103 (2005) 1481.
- [32] H.P. Gunawardena, M. He, P.A. Chrisman, S.J. Pitteri, J.M. Hogan, B.D.M. Hodges, S.A. McLuckey, *J. Am. Chem. Soc.* 127 (2005) 12627.
- [33] S.J. Pitteri, P.A. Chrisman, J.M. Hogan, S.A. McLuckey, *Anal. Chem.* 77 (2005) 1831.
- [34] P.B. O'Connor, C. Lin, J.J. Cournoyer, J.L. Pittman, M. Belyayev, B.A. Budnik, *J. Am. Soc. Mass Spectrom.* 17 (2006) 576.
- [35] C. Lin, P.B. O'Connor, J.J. Cournoyer, *J. Am. Soc. Mass Spectrom.* 17 (2006) 1605.
- [36] M.A. Belyayev, J.J. Cournoyer, C. Lin, P.B. O'Connor, *J. Am. Soc. Mass Spectrom.* 17 (2006) 1428.
- [37] C. Dezarnaud-Dandine, F. Bournel, M. Troncy, D. Jones, A. Modelli, *J. Phys. B: At. Mol. Opt. Phys.* 31 (1988) L492.
- [38] NIST Chemistry WebBook, NIST Standard Database 69, January, 2005. <http://webbook.nist.gov/chemistry/>.